Letter

The rate of the astrophysical ^{48}Cr$(p, \gamma)^{49}$Mn reaction and its influence on the potential $A = 48$ waiting point in the rp process

C. O'Shea [a],[*], G. Lotay [a], D.T. Doherty [a], D. Seweryniak [b], R. Lau [c,d], G. Bartram [a], S. Byrne [e], L. Canete [a], M.P. Carpenter [b], K.A. Chipps [f], P.A. Copp [b,1], C. Cousins [a], J. Henderson [a], T. Huang [c], H. Jayatissa [b,1], F. Kondev [b], C. Müller-Gatermann [b], S.D. Pain [f], C. Paxman [a], B.J. Reed [a], W. Reviol [b], A.M. Rogers [e], R. Russell [a], H. Schatz [d,g], M. Siciliano [b]

[a] *University of Surrey, Guildford, GU2 7XH, United Kingdom*
[b] *Argonne National Laboratory, Argonne, IL 60439, USA*
[c] *Institute of Modern Physics, Chinese Academy of Sciences, Lanzhou 730000, China*
[d] *Facility for Rare Isotope Beams, Michigan State University, East Lansing, MI 48824, USA*
[e] *University of Massachusetts Lowell, Lowell, MA 01854, USA*
[f] *Oak Ridge National Laboratory, Oak Ridge, TN 37831, USA*
[g] *Michigan State University, East Lansing, MI 48824, USA*

ARTICLE INFO

ABSTRACT

We have performed a detailed γ-ray spectroscopy study of the nucleus, ^{49}Mn, using the GRETINA tracking array and FMA recoil separator. With this powerful new setup, low-spin excited states, which are most relevant for astrophysical processes, have been identified for the first time, including four proton-unbound levels, corresponding to key astrophysical resonances in the ^{48}Cr$(p, \gamma)^{49}$Mn reaction. Of these four levels, two were found to dominate the ^{48}Cr$(p, \gamma)^{49}$Mn reaction for temperatures, $T = 0.2 - 1.4$ GK, and uncertainties in the rate have been reduced by more than 3 orders of magnitude. Specifically, γ decays were observed from $1/2^+$ and $3/2^-$ excited states at $E_x = 2570.9(26)$ keV and $2595.8(21)$ keV, corresponding to an $\ell = 0$ and $\ell = 1$ resonance in the ^{48}Cr $+ p$ system at $E_r = 482.9(84)$ keV and $507.9(83)$ keV, respectively. Present simulations of Type-I X-ray burst nucleosynthesis indicate that the newly defined ^{48}Cr(p, γ) reaction rate is sufficiently fast to drive the flow of material towards higher masses in such environments. Consequently, despite the relatively long half life of ^{48}Cr, we now do not expect a strong waiting point in the rp process at $A = 48$.

Type-I X-ray bursts (XRBs) are among the most frequently observed stellar explosions to occur in our Galaxy [1,2]. These violent astronomical events comprise a main sequence star and a neutron star in a close binary system, in which hydrogen- and helium-rich material is accreted onto the compact object from the larger companion. The accreted fuel causes a rapid heating of the neutron star surface and, after several hours to days, a thermonuclear runaway ensues, culminating in a luminous burst of X-rays. Advances in observations, especially in the cases of regular bursting episodes where multiple bursts can be averaged, are now providing X-ray burst light curves at the few % accuracy level. For example, uncertainties for the burst profile of GS 1826-24 in the September 2001 epoch are of the order of 3% [3]. Careful comparisons of the resulting light curves with theoretical models allow for the be-

haviour of matter under extreme conditions to be investigated, and may provide constraints on key neutron star properties; such as the equation-of-state and the mass-radius ratio [4]. Unfortunately, theoretical models of XRB light curves are extremely sensitive to largely unknown nuclear physics information, such as nuclear reaction rates [4–8]. Thus, in order to fully describe XRB light curves, it is essential that we obtain experimental data on the nuclear reactions that govern both the pathway of nucleosynthesis and energy generation in such environments.

XRBs are powered by a sequence of nuclear reactions known as the rp (rapid proton) process − a series of (p, γ) captures and subsequent β^+ decays, synthesizing elements up to the Sn − Te mass region [9]. This is a complex reaction network involving hundreds of nuclei from stable isotopes to the proton dripline (the limit beyond which nuclei are un-

bound with respect to proton emission). With recent advancements in computational power, it has become possible to construct detailed models of the rp-process nucleosynthesis and study the influence of nuclear reaction rate uncertainties [6,7]. In particular, it has been shown that reactions around "waiting-point" nuclei have a significant effect on XRB light curves. These nuclei are defined as points whereby fast proton capture reactions are impeded and the rp process stalls until a much slower β^+ decay or α-capture enables a bypass. Typically, this occurs when a $(p, \gamma) - (\gamma, p)$ equilibrium is reached, and several such cases have been investigated [10–16]. However, an alternative scenario arises when the rate of a (p, γ) reaction on a long-lived nucleus is particularly slow in comparison to the corresponding, competing β decay. In this regard, it has been suggested that the nucleus ^{48}Cr ($t_{1/2} \sim 22$ hrs), which lies on the rp-process path, may represent a previously unexpected waiting point in XRB nucleosynthesis between the doubly-magic nuclei, ^{40}Ca and ^{56}Ni [17]. Due to its long half-life, ^{48}Cr is effectively stable on the timescale of the burst and, therefore, the ^{48}Cr$(p, \gamma)^{49}$Mn reaction is the only way for the flow of material to proceed. In Ref. [7], Cyburt et al. investigated the dependence of XRB nucleosynthesis on uncertainties in (p, γ), (α, γ), and (α, p) nuclear reaction rates, using a $1-$D multizone model that accounted for feedback between changes in nuclear energy generation and changes in astrophysical conditions. In that work, uncertainties in the ^{48}Cr$(p, \gamma)^{49}$Mn reaction were highlighted as having a strong effect on both the XRB light curve and the products of nucleosynthesis, due to the prominent role of the reaction in pushing material beyond the ^{48}Cr bottleneck. Unfortunately, almost no experimental information exists on the ^{48}Cr$(p, \gamma)^{49}$Mn reaction and its rate over the temperature range of XRBs currently carries an overall uncertainty of 10^4 – this is the level of uncertainty that has previously been found, and is often adopted in sensitivity studies, for proton capture rates with unknown resonance energies, and a small number of contributing resonances [18,19].

The ^{48}Cr(p, γ) reaction is expected to be dominated by the contribution of resonant capture to excited states located above the proton-emission threshold energy in ^{49}Mn of 2088(8) keV [20]. In particular, those states that correspond to low-ℓ captures on the 0^+ ground state of ^{48}Cr. Previous studies of the nucleus ^{49}Mn have focused on high-spin states [21], as such levels are strongly populated in fusion-evaporation reactions. However, high-spin states have no influence on the ^{48}Cr(p, γ) stellar reaction rate and, consequently, all excited states of relevance for XRB nucleosynthesis in ^{49}Mn are still to be identified. In this letter we present a new, high-precision, γ-ray spectroscopy study that employs a heavy-ion fusion-evaporation reaction to simultaneously populate excited states in the astrophysically important nucleus ^{49}Mn and its well-studied mirror analog, ^{49}Cr [22]. Mirror nuclei are expected to exhibit nearly identical structures [23] and, as such, by studying the γ decays of both ^{49}Mn and ^{49}Cr with the advanced γ-ray tracking array GRETINA [24], we have been able to make the first identification of ^{48}Cr + p resonant states up to energies $E_r \lesssim 900$ keV, reducing uncertainties in the rate of the ^{48}Cr(p, γ) reaction by ~3 orders of magnitude. This technique has previously been successful for the study of particle-unbound levels in key astrophysical nuclei [25–30]. However, in this case, a key challenge relates to a need to resolve weakly-populated low-spin states from a sea of decay transitions from strongly-populated high-spin levels, for which the coupling of GRETINA with the Argonne Fragment Mass Analyzer (FMA) [31] offered a number of unique experimental advantages. Namely, it provided a high count rate capability, a large solid angle for recoil detection, a high efficiency for high-energy γ rays and significant segmentation, resulting in improved Doppler reconstruction. The above is critical for the observation of low-intensity γ decays.

Here, a ~13-pnA, 75-MeV beam of ^{40}Ca ions, produced by the ATLAS accelerator, was used to bombard a ~200 μg/cm^2 thick ^{11}B target for 144 h in order to produce ^{49}Mn nuclei via the $2n$ evaporation channel. Prompt γ rays were detected using the GRETINA tracking array which, in this instance, consisted of 12 modules, in coincidence with $A = 49$, charge state 18^+ recoils, transmitted to the focal plane of

Table 1

Properties of observed excited states in ^{49}Mn, together with a matching to proposed mirror analogs in ^{49}Cr [22].

E_x (keV)	E_γ (keV)	J^π	Mirror E_x [22] (keV)
0[a]	-	$5/2^-$	0
261.4(1)[a]	261.4(1)	$7/2^-$	272
1059.1(3)[a]	797.4(1)	$9/2^-$	1084
	1059.4(4)		
1541.0(4)[a]	482.1(1)	$11/2^-$	1562
	1279.3(1)		
1681.6(15)	1681.6(15)	$1/2^-$	1703
1742.8(21)	1481.4(20)	$3/2^-$	1741
1935.4(22)	253.8(16)	$3/2^+$	1982
2400.3(29)	466.1(18)	$5/2^+$	2432
	2399.1(30)		
2480.5(6)[a]	939.8(1)	$13/2^-$	2500
	1421.0(2)		
2484.4(19)	2484.3(19)	$7/2^-$	2503
2570.9(26)	633.6(20)	$1/2^+$	2578
	891.2(22)		
2595.9(21)	2595.8(21)	$3/2^-$	2613
(2964.4(28))	(2964.3(28))	$(7/2^+)$	2912

[a] Previously reported in Ref. [22].

the FMA. The focal plane position was determined with a position-sensitive multi-wire proportional counter (MWPC) and ^{49}Mn and ^{49}Cr nuclei were cleanly resolved from $E - \Delta E$ information in a subsequent ionisation chamber, filled with isobutane at a pressure of 12 Torr. Corresponding γ-ray energy and efficiency calibrations were carried out using standard ^{56}Co, ^{88}Y, and ^{152}Eu γ-ray sources (identical tracking conditions [32] were used for both calibration and experimental data). Tracked γ-ray singles data and γ-γ coincidence matrices, gated on the MWPC and ionisation chamber, were produced and analysed in order to obtain information on the ^{49}Mn and ^{49}Cr decay schemes.

Table 1 presents the level energies, γ-ray transition energies, and spin-parity assignments for observed excited states in ^{49}Mn, together with a matching to proposed mirror analogs in the nucleus, ^{49}Cr [22], while Fig. 1 shows the low-lying level structures of the $T = 1/2$, $A = 49$ mirror pair observed in the present study. Previous evaluations of the level structure of ^{49}Mn have only reported four excited states below $E_x = 3$ MeV at 261.38(13), 1059.18(24), 1541.31(25) and 2481.3(4) keV with $7/2_1^-$, $9/2_1^-$, $11/2_1^-$ and $13/2_1^-$ spin-parity assignments, respectively [22]. The earlier reported level energies, as well as known decay transitions, are well reproduced here, and we match such states to $7/2_1^-$, $9/2_1^-$, $11/2_1^-$ and $13/2_1^-$ levels in ^{49}Cr at 271.72(16), 1083.6(3), 1562.1(3) and 2500.1(4) keV, respectively. In addition to the four previously observed excited states, we report the observation of three new bound states in ^{49}Mn at 1681.6(15), 1742.8(21) and 1935.4(22) keV. The newly-observed 1682- and 1743-keV levels were observed to exhibit distinctive, single γ-ray transitions to the ground and the first excited state, respectively, while the 1935-keV state was found to only decay via a 253.8(16)-keV γ ray to the 1682-keV level, as shown in Fig. 2. In comparison with the mirror nucleus, ^{49}Cr, over the energy range $E_x = 1600 - 2100$ keV, both the $1/2_1^-$, 1703.2(4)-keV and $3/2_1^-$, 1741.4(3)-keV states are known to exhibit large γ-decay branches to the ground state. However, only the $3/2_1^-$, 1741-keV level is known to also decay to the first excited state. Furthermore, the $3/2_1^+$, 1981.8(3)-keV excited state in ^{49}Cr is the only level in the range $E_x = 1600 - 2100$ keV to exhibit a decay branch to the $1/2_1^-$, 1703-keV state. As such, we assign the presently observed 1682-, 1743- and 1935-keV excited states in ^{49}Mn as $1/2_1^-$, $3/2_1^-$ and $3/2_1^+$ levels, respectively.

In considering Fig. 2 further, a γ-ray transition to the $1/2_1^-$, 1682-keV level is observed at 891.2(22) keV, indicating an unbound excited state in ^{49}Mn at 2570.9(26) keV. An evaluation of the mirror nucleus, ^{49}Cr, over the energy range, $E_x = 2.0 - 3.0$ MeV, reveals that only the $1/2_1^+$, 2578.1(5)-keV level is known to exhibit a 875.3(6)-keV decay
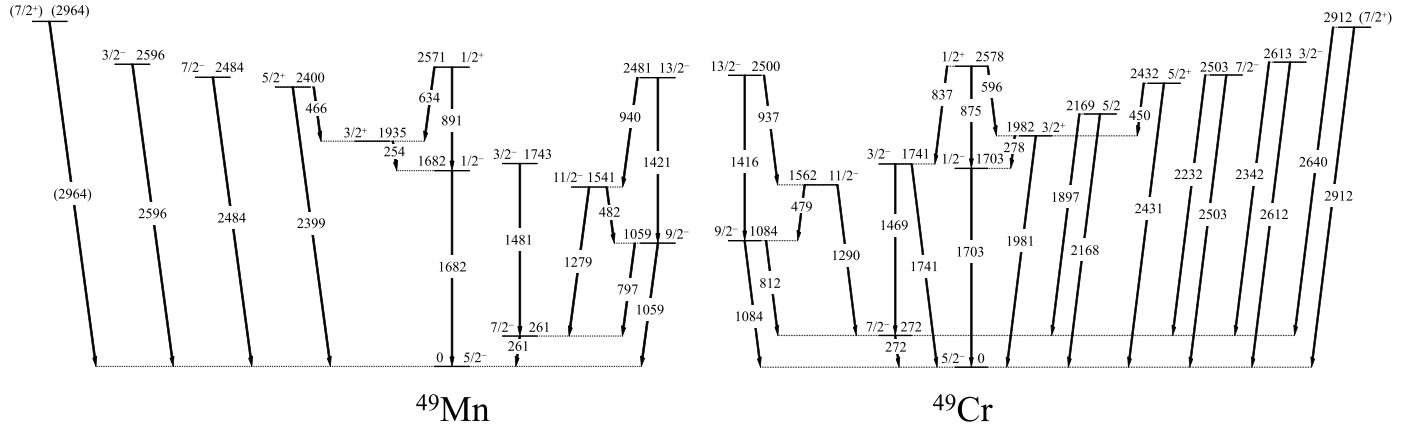
Fig. 1. Low-lying level structures of the mirror nuclei ^{49}Mn and ^{49}Cr observed in the present study.
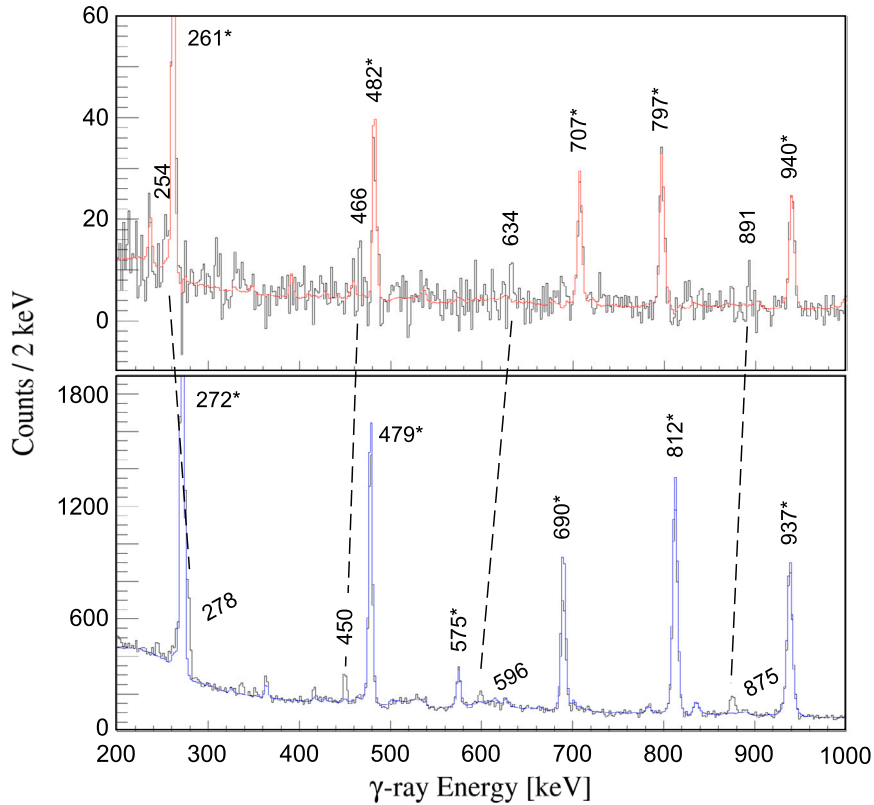

Fig. 2. (top) $\gamma-\gamma$ coincidence spectrum with a gate placed on the newly observed 1682-keV, $1/2_1^- \rightarrow 5/2_1^-$ transition in ^{49}Mn. Observed within the gate are a significant number of coincidences from Compton-scattered, higher-energy transition events originating from strongly populated high-spin states. As such, events coincident with the gate are shown in black, while a scaled projection of the total matrix, which highlights high-spin states, is shown in red. Known transitions from high-spin states have been marked with an asterisk. (bottom) $\gamma-\gamma$ coincidence spectrum with a gate placed on the analog 1703-keV, $1/2_1^- \rightarrow 5/2_1^-$ transition in ^{49}Cr. In similarity with the above, events coincident with the gate are shown in black, while a scaled projection of the total matrix is shown in blue. Known transitions from high-spin states have been marked with an asterisk. Dashed lines between ^{49}Mn and ^{49}Cr spectra denote analog transitions from mirror states.

branch to the $1/2_1^-$ excited state [22], which is also observed in the present work (see Fig. 2). An additional branch to the lower-lying $3/2_1^+$ level has also been reported for the $1/2^+$, 2578-keV state in ^{49}Cr [22], and, here, we observe this decay at 596(1) keV, as illustrated in Fig. 2 (note that the $3/2_1^+$ state feeds the $1/2_1^-$ level via a 254-keV γ ray). In the current data, we observe a similar 633.6(20)-keV decay to the $3/2_1^+$ excited state in ^{49}Mn, in good agreement with the existence of an unbound excited state at 2571 keV. Consequently, we assign the presently observed 891- and 634-keV transitions to originate from a $1/2_1^+$, 2571-keV level in ^{49}Mn.

Fig. 3 displays the tracked γ-ray singles spectrum of ^{49}Mn over the energy range, $E_\gamma = 2200 - 3200$ keV, in which three high-energy direct-to-ground state transitions in ^{49}Mn can be seen at 2399.1(30), 2484.3(19) and 2595.8(21) keV, respectively. Also shown in Fig. 3 is the corresponding analog tracked γ-ray singles spectrum of ^{49}Cr. Here, we observe similar known direct-to-ground state transitions at 2431(1), 2503(1) and 2612(1) keV from the $5/2_1^+$, $7/2_2^-$ and $3/2_2^-$ excited states in ^{49}Cr, respectively [22]. Consequently, based on mirror energy differences observed in the present study, we assign the presently observed excited states in ^{49}Mn at 2400, 2484 and 2596 keV

Table 2
Parameters of ^{48}Cr + p resonances in ^{49}Mn [S_p = 2088(8) keV [20]]. Gamma-ray partial widths have been determined from the lifetimes of mirror analog states in ^{49}Cr [22], where available, and proton partial widths have been evaluated using spectroscopic factors, C^2S, presented. For the $1/2^+$ resonance, no lifetime information is known. As such, we have adopted a half-life of 0.8 ps, based on the known half-life of a $E_x \sim 2.7$ MeV, $1/2^+$ state in the nearby nucleus, ^{53}Mn [36]. See text for details on the assumed uncertainties for proton and γ-ray partial widths.

E_x (keV)	E_r (keV)	J^π	C^2S	Γ_p (eV)	Γ_γ (eV)	$\omega\gamma$ (eV)
2400.3(29)	312.3(85)	$5/2^+$	0.01	7.90×10^{-11}	6.91×10^{-4}	2.37×10^{-10}
2484.4(19)	396.4(82)	$7/2^-$	0.01	3.71×10^{-10}	5.70×10^{-2}	1.48×10^{-9}
2570.9(26)	482.9(84)	$1/2^+$	0.03	3.89×10^{-5}	5.70×10^{-4}	3.64×10^{-5}
2595.9(21)	507.9(83)	$3/2^-$	0.01	1.24×10^{-5}	1.01×10^{-2}	2.48×10^{-5}
2964.4(28)	876.4(85)	$7/2^+$	0.01	3.35×10^{-6}	8.77×10^{-4}	1.34×10^{-5}

as the $5/2_1^+$, $7/2_2^-$ and $3/2_2^-$ levels, respectively. An additional high-energy, direct-to-ground state, decay transition at 2964.4(28) keV in ^{49}Mn is tentatively observed in the current data, as shown in Fig. 3, and we propose here a matching with the $7/2_1^+$, 2911.7-keV excited state in the analog nucleus, ^{49}Cr, which is known to exhibit a strong γ-decay branch to the ground state [22].
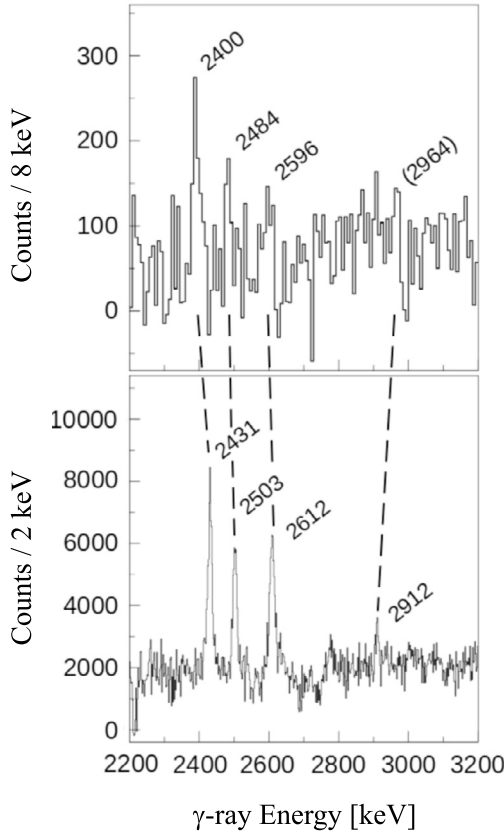

Fig. 3. (top) Tracked γ-ray singles spectrum of ^{49}Mn over the energy range, $E_\gamma = 2200 - 3200$ keV, with a condition placed on multiplicity 1 events. Multiplicities of 4 and higher, corresponding to high-spin events, have been subtracted from the spectrum. (bottom) Tracked γ-ray singles spectrum of ^{49}Cr over the energy range $E_\gamma = 2200 - 3200$ keV, with the same multiplicity condition as above. Dashed lines between ^{49}Mn and ^{49}Cr spectra denote analog transitions from mirror states.

For a new evaluation of ^{48}Cr$(p,\gamma)^{49}$Mn stellar reaction rate, we use resonance energies and spin-parity assignments, determined in the present work, and adopt proton spectroscopic factors, C^2S, of 0.01 for all resonances with the exception of the key, $1/2_1^+$, 2571-keV $\ell = 0$

state. For the latter, we use the $C^2S = 0.03$ reported for a similar $1/2_1^+$, 2275.9(2)-keV excited state in ^{51}Mn, populated via the ^{50}Cr$(^3$He,$d)$ reaction [33]. It is likely that the 2571-keV state in ^{49}Mn has a similar structure to the 2276-keV excited level in ^{51}Mn, and any shell-model calculations for such a state would be very challenging (since such a calculation for an intruder state would extend outside of the standard fp valence space). Furthermore, we note that $7/2^-$, $3/2^-$ and $5/2^+$ excited states in ^{51}Mn at $E_x \sim 2.4$, 2.9 and 3.0 MeV, respectively, have all been reported to have proton spectroscopic factors, C^2S, of 0.01 [33], which gives some confidence that our choice of C^2S values for resonant states in ^{49}Mn is reasonable.

Proton partial widths were then determined using the formalism of Ref. [34]. This has been shown to reproduce experimentally known proton partial widths to within a factor ~ 1.7 [35], and, as such, we assume a relatively conservative overall uncertainty in the determination of proton partial widths of a factor ~ 2. In almost all cases, the proton partial widths of ^{48}Cr + p resonant states are significantly smaller that the corresponding γ-ray partial widths. As such, uncertainties in γ-ray partial widths are expected to be negligible. In the case of the $\ell = 0$, 2571-keV state, in which the proton and γ-ray partial widths are comparable, we assume a γ-ray partial width uncertainty of a factor ~ 2. Finally, in order to account for the propagation of uncertainties in resonance strengths and thus, the total stellar reaction rate, barrier penetrabilities were determined for both the low and high values of the resonance energy for each state. The resulting proton partial widths (calculated using the formalism of Ref. [34]) were then varied within their assumed uncertainty of a factor of ~ 2 to obtain estimates for low and high resonance strengths. A complete list of resonance parameters used for the estimation of the ^{48}Cr$(p,\gamma)^{49}$Mn stellar reaction rate is provided in Table 2.

Based on our present evaluation of the ^{49}Mn reaction, we find that the newly observed $\ell = 0$ resonance at $E_r = 482.9(84)$ keV dominates the entire rate over the temperature range $T = 0.2 - 1.4$ GK, with a significant contribution from the $\ell = 1$, 507.9(83)-keV resonance. Uncertainties in the newly determined resonance energies alone, ~ 8 keV, result in only $\sim 30\%$ changes in the overall rate. However, combined with uncertainties in both proton partial widths and γ-ray partial widths, these result in factors of $\sim 5 - 10$ variations in resonance strength estimations. Consequently, we deduce that uncertainties in the ^{48}Cr$(p,\gamma)^{49}$Mn reaction have now been reduced by more than 3 orders of magnitude, shown in Fig. 4.

To assess the astrophysical implications of the present work on XRB nucleosynthesis, we have performed a series of calculations using the stellar modelling code, MESA [5,37], in which the rate of the ^{48}Cr$(p,\gamma)^{49}$Mn reaction was varied within its previous 10^4 uncertainty band (taken as the REACLIB [38] nominal rate $\times 100$ and $/100$, respectively). Fig. 5(a) shows the composition of the final burst ashes and waiting points can be readily identified by their associated abundance peaks. It is evident that if the previous low ^{48}Cr(p,γ) rate is adopted, a
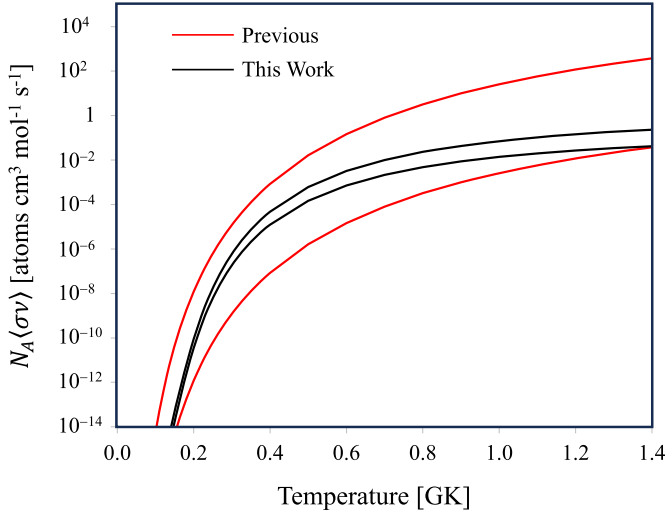
Fig. 4. The ^{48}Cr(p,γ) stellar reaction rate over the temperature range $T = 0-1.4$ GK. The presently determined rate estimated by resonance parameters provided in Table 2 is shown in black, while the previous estimation of rate uncertainties is shown in red. It is important to note that present calculations of the stellar reaction rate likely represent a lower limit, particularly at high temperatures, $T \gtrsim 1$ GK, as higher-lying, unobserved resonances may also contribute.

now require a more precise mass measurements of ^{48}Cr and ^{49}Mn, as well as an experimental determination of proton spectroscopic factors of key resonant states. The latter could be obtained via a study of neutron spectroscopic factors in the mirror nucleus, ^{49}Cr, using the ^{48}Cr(d,p) single-nucleon transfer reaction. However, it is important to note that the ^{48}Cr(p,γ) reaction is only important for XRB nucleosynthesis if its rate is very low, and, at present, our low rate likely represents a lower limit for the rate.
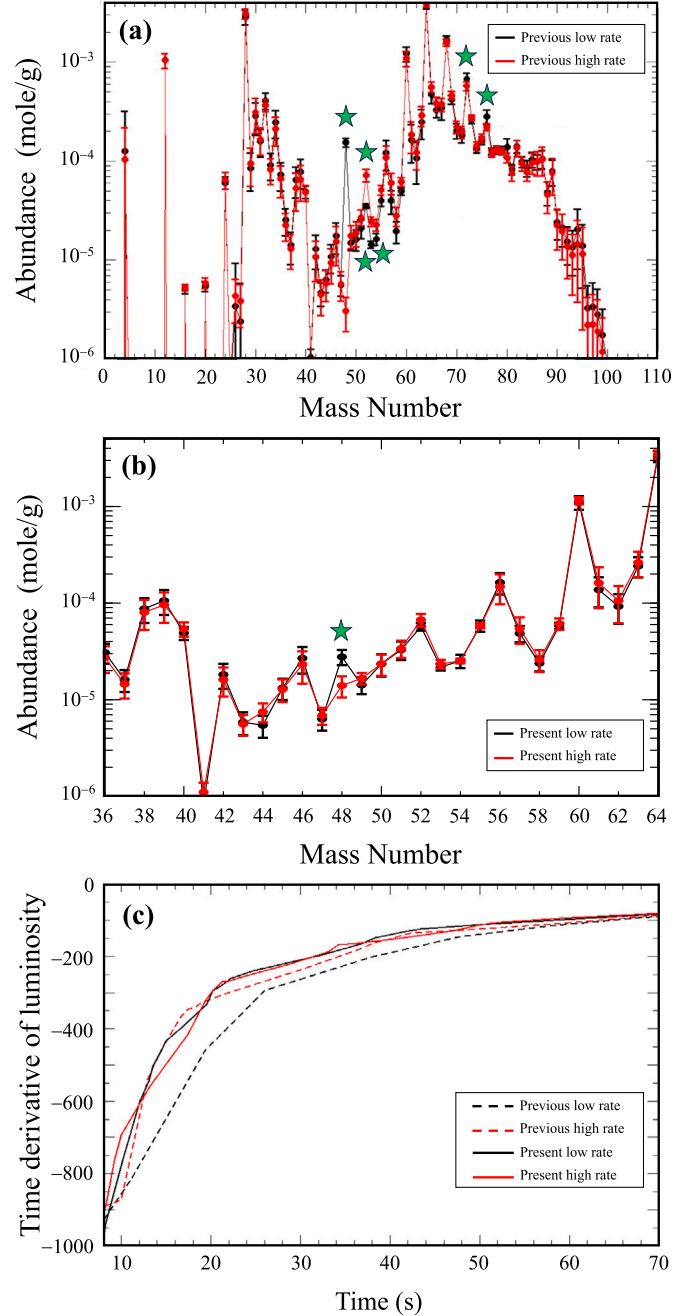
new waiting point in the *rp* process would exist at $A = 48$, and significant variations in the abundance of $A = 52 - 54$, 72, and 76 isotopes would occur. This would also strongly affect the tail of the XRB light curve from which all critical neutron star properties, such as the mass-radius ratio, may be extracted [4]. In particular, we find that the burst luminosity in the tail of the light curve may vary by up to 6%, which is significant compared to observational errors of the order 3% [3]. However, the biggest impact of the rate uncertainty is on the slope of the modelled burst tail, shown in Fig. 5(c). Here, the previous low rate results in a change in the slope of the XRB light curve tail of up to 60%. Thus, current calculations confirm that determining whether or not the ^{48}Cr$(p,\gamma)^{49}$Mn reaction affects the composition of the burst ashes is essential for modelling neutron star crusts [39,40] and for predictions of observational signatures of potentially ejected material [41,42]. Consequently, we repeated our MESA burst calculations with the present, experimentally determined, low and high reaction rates, and found that no significant changes were observed in both the average burst light curve and slope of the burst tail. Shown in Fig. 5(c), the resulting slope of the present low and high rate burst light curve is consistent with the slope of the previous high rate burst light curve. This indicates that the impact of the ^{48}Cr(p,γ) rate uncertainty on modelled burst light curves has been removed by our experiment. It should be noted that the lower ^{48}Cr(p,γ) reaction rate from this work still creates an abundance peak at $A = 48$, as shown in Fig. 5(b). However, the peak is more than an order of magnitude smaller than those associated with the known, major waiting points. Our measurements therefore indicate that a significant waiting point at ^{48}Cr can now be excluded.

In summary, we have performed a detailed γ-ray spectroscopy study of the nucleus ^{49}Mn. Low-spin excited states have been identified for the first time, including four new proton-unbound resonant levels, corresponding to key astrophysical resonances in the ^{48}Cr + p system. In particular, an $\ell = 0$ resonance and an $\ell = 1$ resonance were identified at $E_r = 483$ keV and 508 keV, respectively. These states were found to dominate the ^{48}Cr$(p,\gamma)^{49}$Mn stellar reaction rate over the temperature range, $T = 0.2 - 1.4$ GK, reducing uncertainties in the rate by more than 3 orders of magnitude. Current MESA simulations indicate that the newly defined ^{48}Cr(p,γ) reaction rate does not result in a significant overabundance of $A = 48$ nuclei in XRBs. Consequently, we conclude that there is unlikely to be a major waiting point in the *rp* process at $A = 48$. Further constraints on the rate of the ^{48}Cr(p,γ) reaction would

Fig. 5. (a) MESA calculations of the effects of varying the ^{48}Cr(p,γ) reaction rate by its previous associated uncertainties on final isotopic abundances. Significantly affected isotopes have been denoted by green stars. (b) Effects of varying the ^{48}Cr(p,γ) reaction rate by present uncertainties from this work on final isotopic abundances. The abundance peak at $A = 48$ has been denoted by a green star. (c) Time derivative of XRB luminosity as a function of time, for the tail portion of the light curve, using both the previous and present uncertainties in the ^{48}Cr$(p,\gamma)^{49}$Mn reaction rate.

Declaration of competing interest

The authors declare that they have no known competing financial interests or personal relationships that could have appeared to influence the work reported in this paper.

Data availability

Data will be made available on request.

References

[1] W.H.G. Lewin, J. van Paradijs, R.E. Taam, Space Sci. Rev. 62 (1993) 223.
[2] H. Schatz, K. Rehm, Nucl. Phys. A 777 (2006) 601.
[3] D.K. Galloway, A.J. Goodwin, L. Keek, Astrophys. Publ. Astron. Soc. Austral. 34 (2017) 19.
[4] Z. Meisel, G. Merz, S. Medvid, Astrophys. J. 872 (2019) 84.
[5] Z. Meisel, Astrophys. J. 860 (2018) 147.
[6] A. Parikh, J. Jose, F. Moreno, C. Iliadis, Astrophys. J. Suppl. Ser. 178 (2008) 110.
[7] R.H. Cyburt, et al., Astrophys. J. 830 (2) (2016) 55.
[8] A. Parikh, J. José, C. Iliadis, F. Moreno, T. Rauscher, Phys. Rev. C 79 (2009) 045802.
[9] R.K. Wallace, S.E. Woosley, Astrophys. J. Suppl. Ser. 45 (1981) 389.
[10] H. Jayatissa, et al., Phys. Rev. Lett. 131 (2023) 112701.
[11] G. Lotay, et al., Phys. Lett. B 833 (2022) 137361.
[12] J.S. Randhawa, et al., Phys. Rev. Lett. 125 (2020) 202701.
[13] J.S. Randhawa, et al., Phys. Rev. C 104 (2021) L042801.
[14] C. Langer, et al., Phys. Rev. Lett. 113 (2014) 032502.
[15] J. Browne, et al., Phys. Rev. Lett. 130 (2023) 212701.
[16] X. Zhou, et al., Nat. Phys. 19 (2023) 1091.
[17] J.L. Fisker, H. Schatz, F.-K. Thielemann, Astrophys. J. Suppl. Ser. 174 (2008) 261.
[18] R.R.C. Clement, et al., Phys. Rev. Lett. 92 (2004) 2502.
[19] C. Iliadis, et al., Astrophys. J. Suppl. Ser. 142 (2002) 105.
[20] M. Wang, et al., Chin. Phys. C 36 (2012) 1603.
[21] J.A. Cameron, et al., Phys. Lett. B 235 (1990) 3.
[22] T.W. Burrows, Nucl. Data Sheets 109 (2008) 1879.
[23] D.D. Warner, M.A. Bentley, P. Van Isacker, Nature (London) 2 (2006) 311.
[24] S. Paschalis, et al., Nucl. Instrum. Methods Phys. Res., Sect. A 709 (2013) 44.
[25] D. Seweryniak, et al., Phys. Lett. B 590 (2004) 170.
[26] D. Seweryniak, et al., Phys. Rev. Lett. 94 (2005) 032501.
[27] D. Seweryniak, et al., Phys. Rev. C 75 (2007) 062801(R).
[28] G. Lotay, et al., Phys. Rev. C 77 (2008) 042802(R).
[29] A.R.L. Kennington, et al., Phys. Rev. Lett. 124 (2020) 252702.
[30] L. Canete, et al., Phys. Rev. C 108 (2023) 035807.
[31] C.N. Davids, J.D. Larson, Nucl. Instrum. Methods Phys. Res., Sect. B 40–41 (1989) 1224.
[32] T. Lauritsen, et al., Nucl. Instrum. Methods Phys. Res., Sect. A 836 (2016) 46.
[33] J.E. Kim, W.W. Daehnick, Phys. Rev. C 23 (1981) 742.
[34] C. Iliadis, Nucl. Phys. A 618 (1997) 166.
[35] C. Iliadis, P.M. Endt, N. Prantzos, W.J. Thompson, Astrophys. J. 524 (1999) 434.
[36] H. Junde, Nucl. Data Sheets 110 (2009) 2689.
[37] B. Paxton, et al., Astrophys. J. Suppl. Ser. 192 (2011) 35.
[38] R.H. Cyburt, et al., Astrophys. J. Suppl. Ser. 189 (2010) 240.
[39] R. Lau, et al., Astrophys. J. 859 (2018) 62.
[40] Z. Meisel, et al., J. Phys. G, Nucl. Part. Phys. 45 (2018) 093001.
[41] N.N. Weinberg, L. Bildsten, H. Schatz, Astrophys. J. 639 (2006) 1018.
[42] Y. Herrera, G. Sala, J. José, Astron. Astrophys. 678 (2023) A156.